SUPPORTING INFORMATION to

Multiple retinal isomerizations during the early phase of the bestrhodopsin photoreaction

Spyridon Kaziannis[1,2¶], Matthias Broser[3¶], Ivo H.M. van Stokkum[4], Jakub Dostal[1], Wayne Busse[3], Arno Munhoven[3], Cesar Bernardo[1], Miroslav Kloz[1], Peter Hegemann[3*], John T.M. Kennis[4*]

[1]ELI-Beamlines, Institute of Physics, Na Slovance 2, 182 21 Praha 8, Czech Republic
[2]Department of Physics, University of Ioannina, Ioannina, Gr-45110
[3]Institut für Biologie, Experimentelle Biophysik, Humboldt Universität zu Berlin, Invalidenstrasse 42, D-10115 Berlin, Germany
[4]Department of Physics and Astronomy, Faculty of Science, Vrije Universiteit Amsterdam, Amsterdam 1081 HV, De Boelelaan 1081, The Netherlands

[¶]these authors contributed equally
*corresponding authors, j.t.m.kennis@vu.nl, hegemann@rz.hu-berlin.de

Supporting text

Origin and character of RSB HOOP modes

In RSB, the HOOP modes consist of linear combinations of the CH and/or NH wag coordinates (1). The methyl groups at C9 and C13 divide the HOOP modes into three vibrationally isolated groups: hydrogens of (i) C7 and C8; (ii) C10, C11, and C12; (iii) C14, C15. and N. Within these groups, the wags couple across the double bonds. The C7H and C8H, the C11H and C12H, and the C15H and NH wags strongly couple, forming in-phase (A_u) and out-of-phase (B_g) normal modes. The C10H and C14H wag coordinates appear as isolated modes (1).

Target analysis of TA data

To identify the absolute spectra of the photointermediates devoid of the GSB component and to quantitatively estimate the product quantum yield, we performed a target analysis in a procedure similar to that applied for the Chrimson channelrhodopsin (2). We assume that only the shortest living excited-state component (1.4 ps) results in the primary photoproduct P1 at a quantum yield of 11%, after which P1 sequentially evolves to P2, P3, P4, and P5, as shown in Fig S3A. Species -associated spectra (SAS) of P1, P2, P3 and P4 are indicated in dark green, black, red, and blue, respectively, in Fig. S3B. Fig S3C shows the temporal concentration profiles. The P1, P2, and P4 SAS attain a reasonable shape, but the P3 SAS is unusually broad and shows a clear shoulder that coincides with the P2 absorption, which suggests an equilibrium existing between P2 and P3. Fig. S3D shows a kinetic scheme where P2 and P3 assume a 1:1 equilibrium with a 1.2 μs time constant. The temporal concentration profile is shown in Fig S3E. The resulting SAS are shown in Fig. 3C in the main text with P1, P2, P3, and P4 indicated in dark green, black, red, and blue, respectively. They show well-separated and defined spectral shapes, strongly suggesting that P2 and P3 indeed exist in an equilibrium. We applied the same model on the flash photolysis data to include the final intermediate P5, which yielded the SAS shown in Fig. 3D in the main text. Their absorption maxima, as determined from a skewed Gaussian fit, are located at 682 nm, 673 nm, 595 nm, 560 nm, and 540 nm, respectively. Henceforth, we refer to the intermediates as P682 (P1), P673 (P2), P595 (P3), P560 (P4), and P540 (P5).

Assignment of HOOP, methyl and C-C stretch modes in P682 and P673

The absolute P673 FSRS spectrum shows HOOP intensity around 960 cm^{-1}, a frequency similar to that observed in BR K (957 cm^{-1}). The shoulder at 940 cm^{-1} was observed as a separate band at 943 cm^{-1} in BR K (3). The 960 cm^{-1} band may be assigned to the HC7=C8H A_u HOOP (4), while the 940 cm^{-1} band may be assigned to the HC11=C12H A_u HOOP, indicating distortions around the C7=C8 and C11=C12 double bonds. The 813 cm^{-1} band (possibly the C14H HOOP mode) was observed in BR K at a moderate amplitude, while the 881 cm^{-1} band (C10H - C11H) was observed at a low amplitude in BR K. The origin of the 844 cm^{-1} band is unclear. In addition to the HOOP bands, the P673 SADS shows a C=C stretch vibrational band at 1503 cm^{-1} consistent with its absorption in the red (5). In the fingerprint region, a large band at 1185 cm^{-1} was observed, indicative of 13-*cis* RSB. It corresponds to the 1190 cm^{-1} band in the difference spectrum (Fig

5C, black line). The methyl rock vibration was upshifted to 1023 cm^{-1}, an unusually high frequency. Only a single methyl rock vibration band was observed as in the BR K intermediate (3, 6), which is an important observation as it implies that the degeneracy of the methyl rock vibration has not been lifted. This finding provides further evidence that P673 mainly corresponds to 13-*cis* RSB.

The P682 SADS shows HOOP bands similar to that of P673, but since it corresponds to a mixture of 13-*cis* and 11-*cis* RSB, it is less straightforward to assign them to specific modes of the two species. Still, one band stands out: the 935 cm^{-1} mode has a larger amplitude in P682 compared to P673, which suggests it belongs to the 11-*cis* conformer. It transforms to the 960 cm^{-1} band in P673. Even if the 935 cm^{-1} cannot be firmly assigned because there has not been an observation before in 11-*cis* species, such as the rhodopsin dark state (7), we will tentatively assign it. In general, HOOP mode frequencies differ only slightly between all-*trans* and 13-*cis* RSB (4), suggesting that such is valid for 11-*cis* as well if the mode is sufficiently far away from the isomerized C11=C12 double bond. In light-adapted BR, a 942 cm^{-1} HOOP mode was assigned to the N-H wag with a contribution from Lys (8). It is possible that the 935 cm^{-1} mode of P682 could be assigned to this N-H wag vibration in 11-*cis* RSB. This possibility would indicate a notable distortion at the N heteroatom. The 935 cm^{-1} mode does not correspond to the HC11=C12H A_u HOOP, since the latter mode is located at 969 cm^{-1} in 11-*cis* RSB (7). In the fingerprint region, the 1185 cm^{-1} band indicative of 13-*cis* RSB dominates the spectrum, while the 1218 cm^{-1} band indicative of 11-*cis* RSB is visible as a shoulder.

Supporting figures

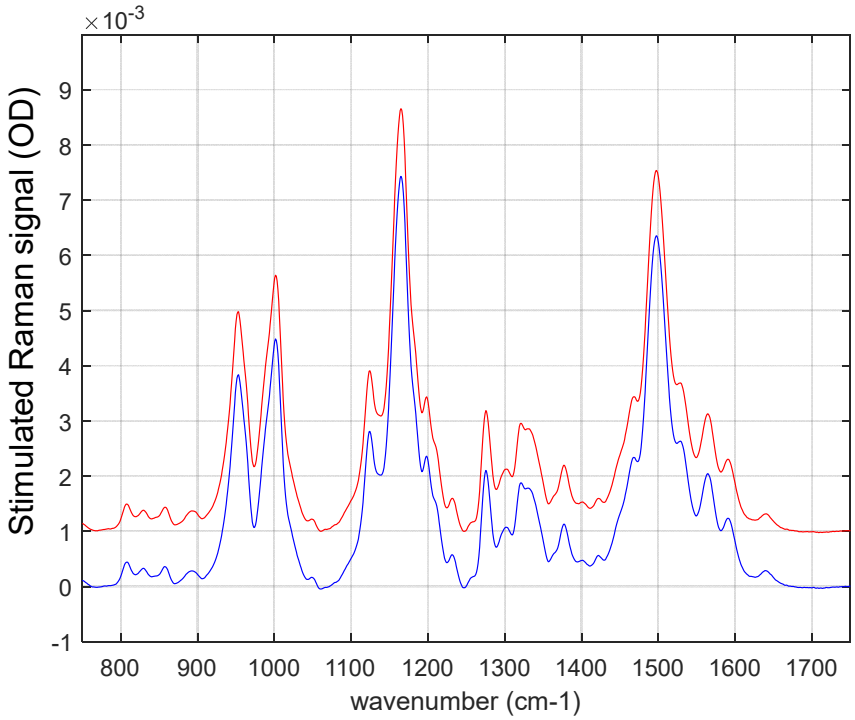

Fig. S1. Ground state stimulated Raman spectra of D661 upon dark relaxation (blue line) and green background illumination (red line).

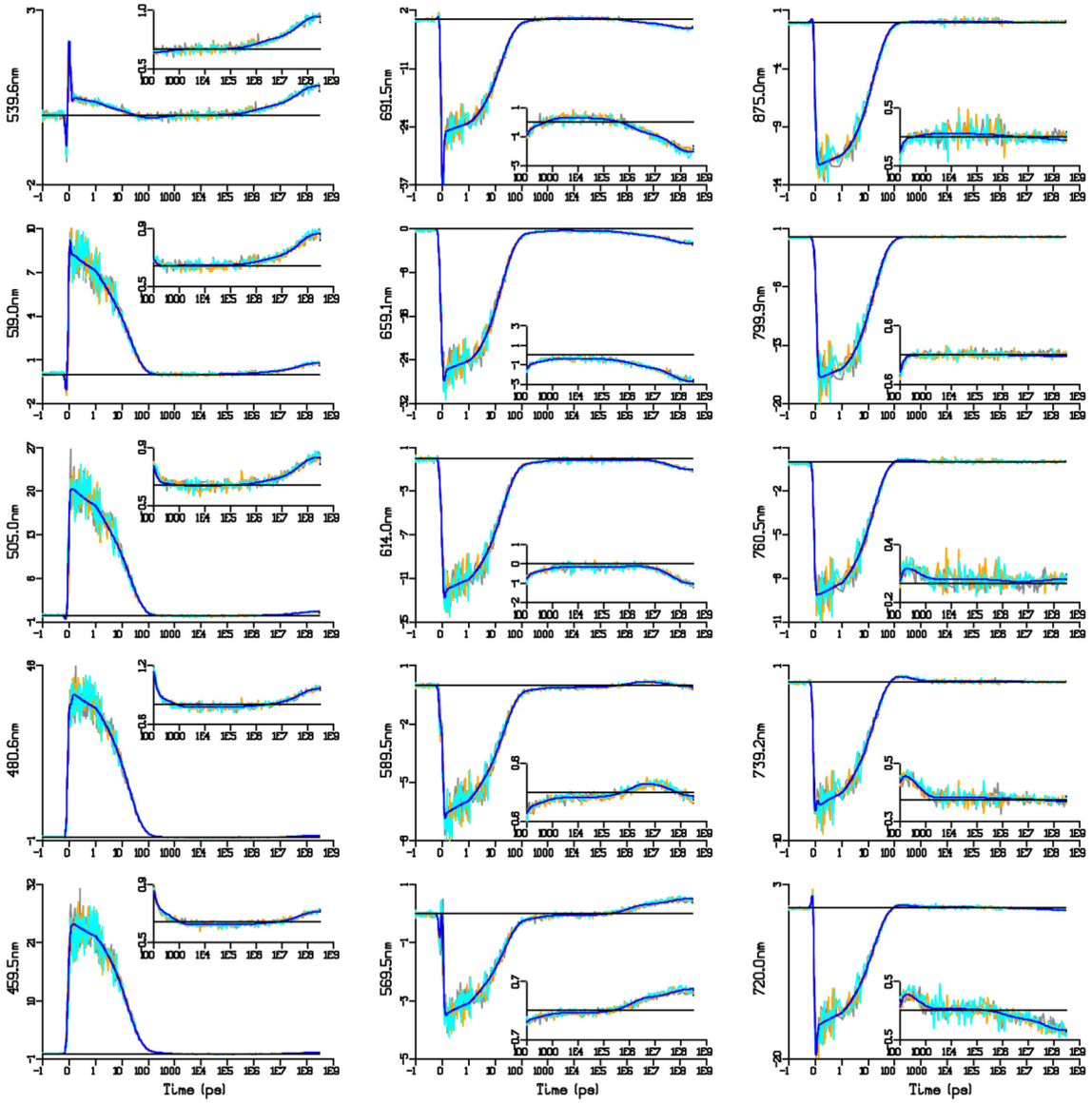

Figure S2. (A) Selected time traces of the bestrhodopsin transient absorption (horizontal axes from fs - sub-ms, vertical axes ΔA in mOD) at 15 wavelengths (indicated in the ordinate label of the panels) after 700 nm excitation. Key: three experiments (grey, orange, cyan). Black, red, and blue lines indicate the simultaneous target analysis fit. The overall rms error of the fit was 0.66 mOD. The time axis is linear until 1 ps and logarithmic thereafter. The insets show the kinetics after zoom after 100 ps to emphasize the product dynamics.

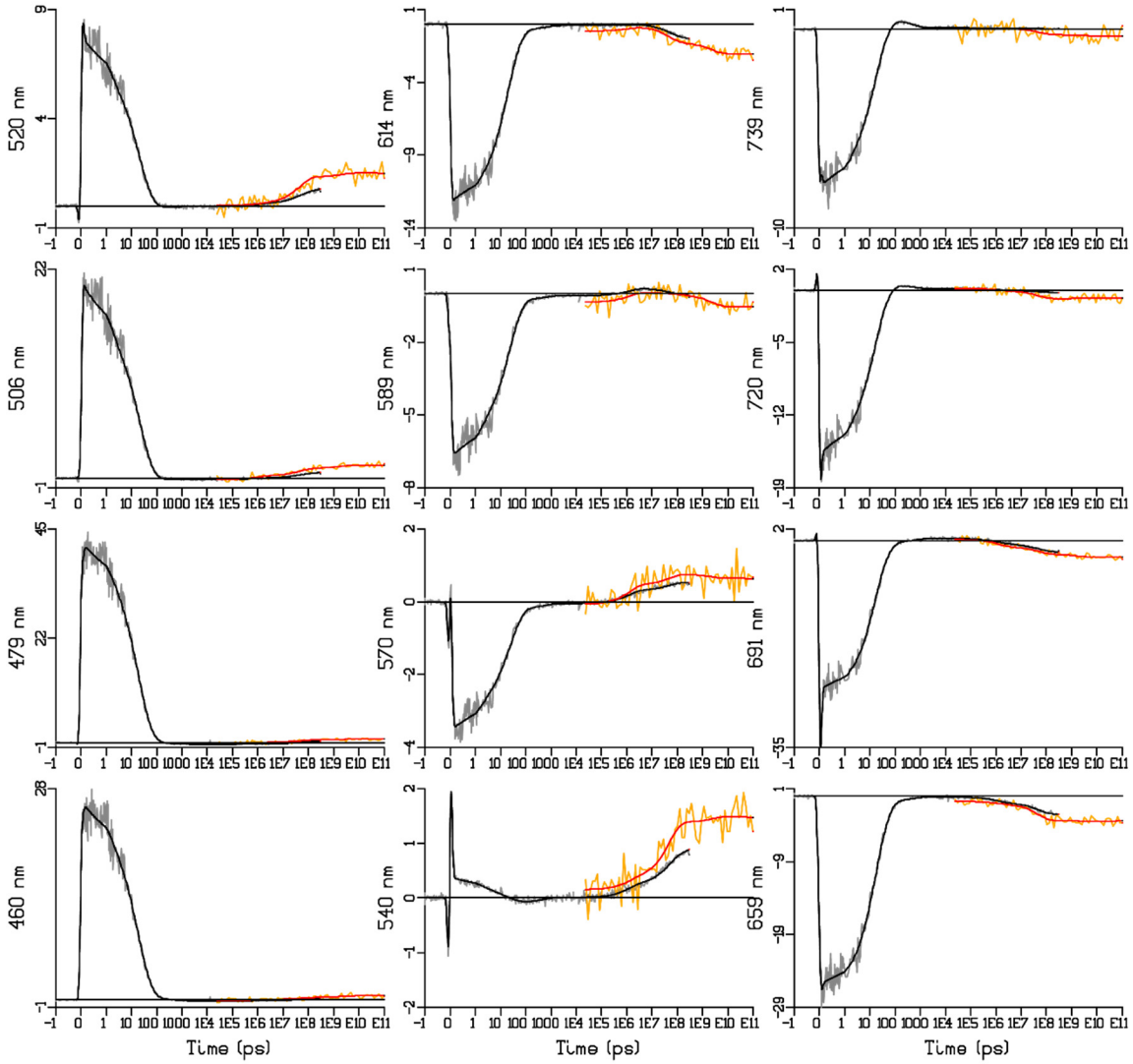

(B) Overlay of flash photolysis data after 660 nm excitation (orange) at 12 wavelengths (indicated in the ordinate label of the panels), horizontal axes from fs - sub-ms, vertical axes ΔA in mOD, with the average of the transient absorption (fs - sub-ms, grey). Black and red lines indicate the simultaneous target analysis fit. The overall rms error of the fit was 0.44 mOD. The time axis is linear until 1 ps and logarithmic thereafter.

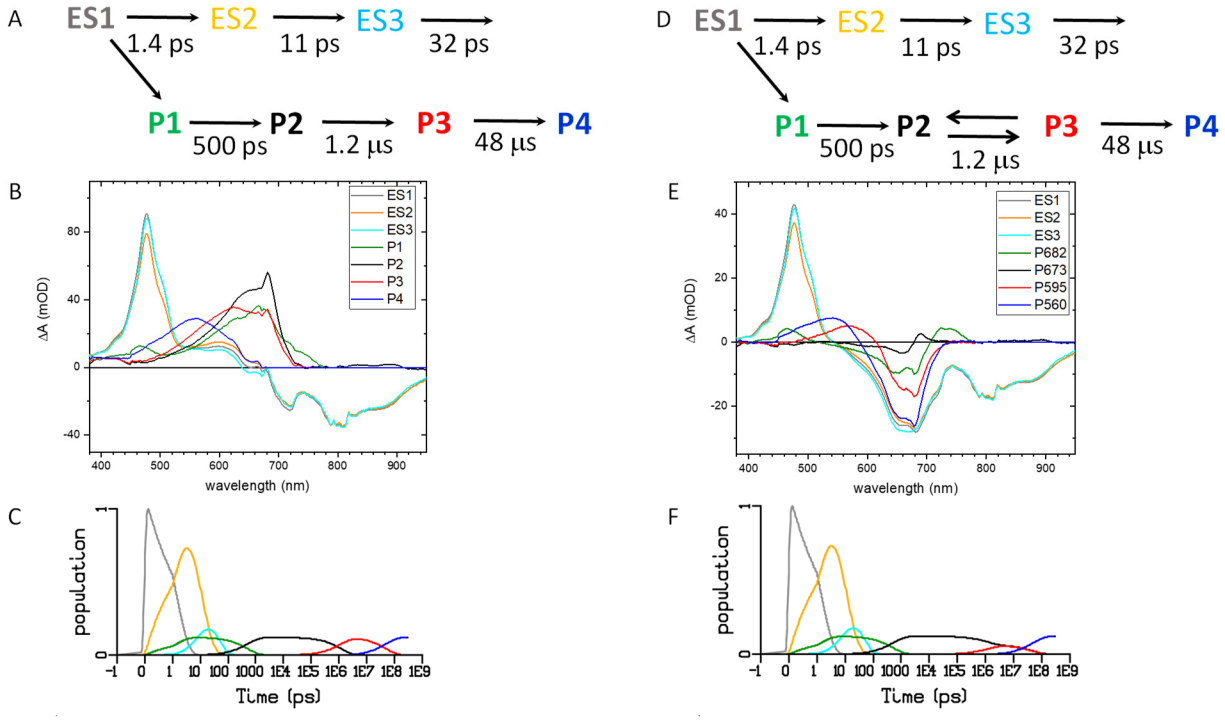

Fig. S3. Target analysis models, SAS, SADS, and concentration profiles of TA data spectra. (A) target analysis scheme with sequential product evolution. The quantum yield of P1 from ES1 is 11%, whereas 89% decays to ES2 in 1.4 ps. 68% of ES2 decays to the ground state (GS), whereas 32% decays to ES3 in 11 ps. In turn, ES3 returns to GS in 32 ps. From the flash photolysis data, it was found that P4 decays in 1.0 ms to the long-lived P5. (B) species-associated spectra (SAS) of TA data were analyzed with the model in panel (A). (C) temporal concentration profile of the SAS based on the kinetic model of panel (A). (D) target analysis scheme with product evolution with P1 = P683, P2 = P673, P3 = P595, and P4 = P560, assuming an equilibrium between P2 (P673) and P3 (P595). (E) species-associated difference spectra (SADS) of TA data analyzed with the model in panel (D). The estimated SAS are depicted in Fig. 3C in the main text. (F) temporal concentration profile of the SAS based on the kinetic model of panel (D).

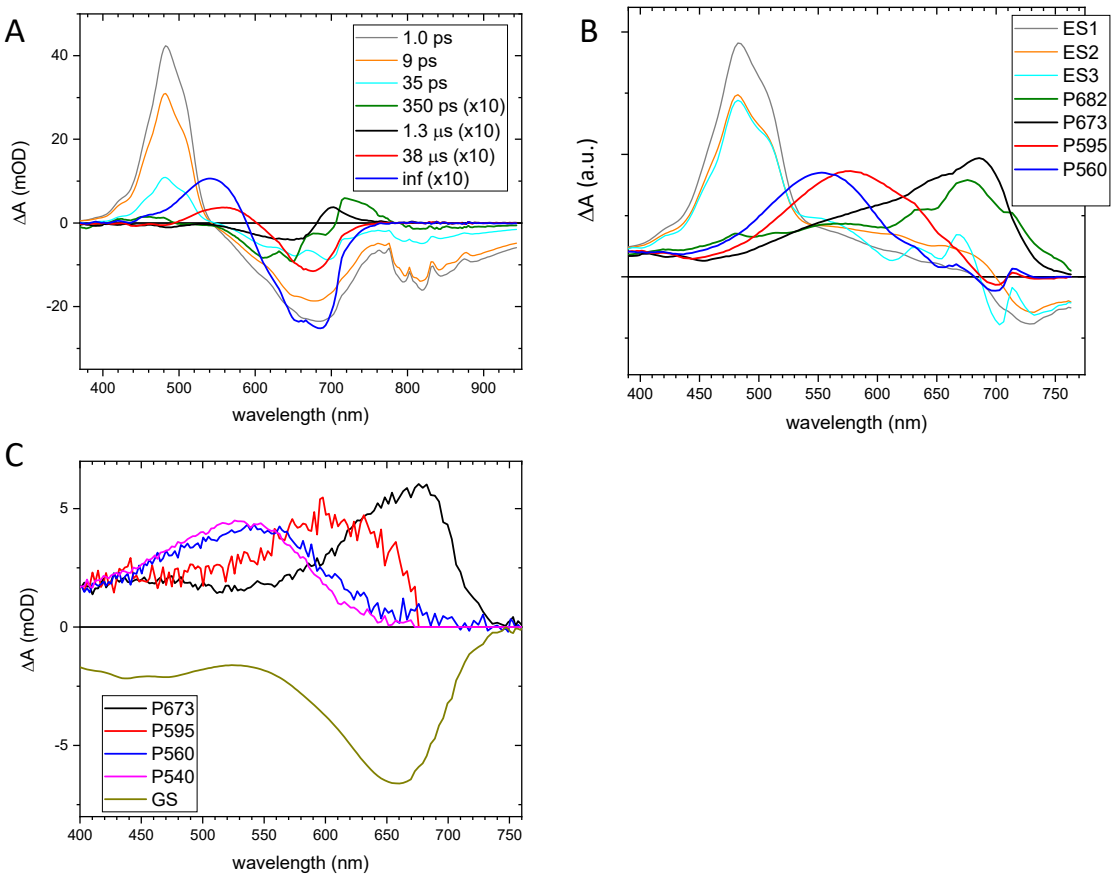

Fig. S4. TA results for the Lys mutant. (A) EADS that follow from a sequential analysis of the TA data for the Lys mutant, with time constants indicated in the panel; (B) SAS that follow from a target kinetic model identical to that in wild type of Fig. S3C. (C) SAS of the flash photolysis data.

D

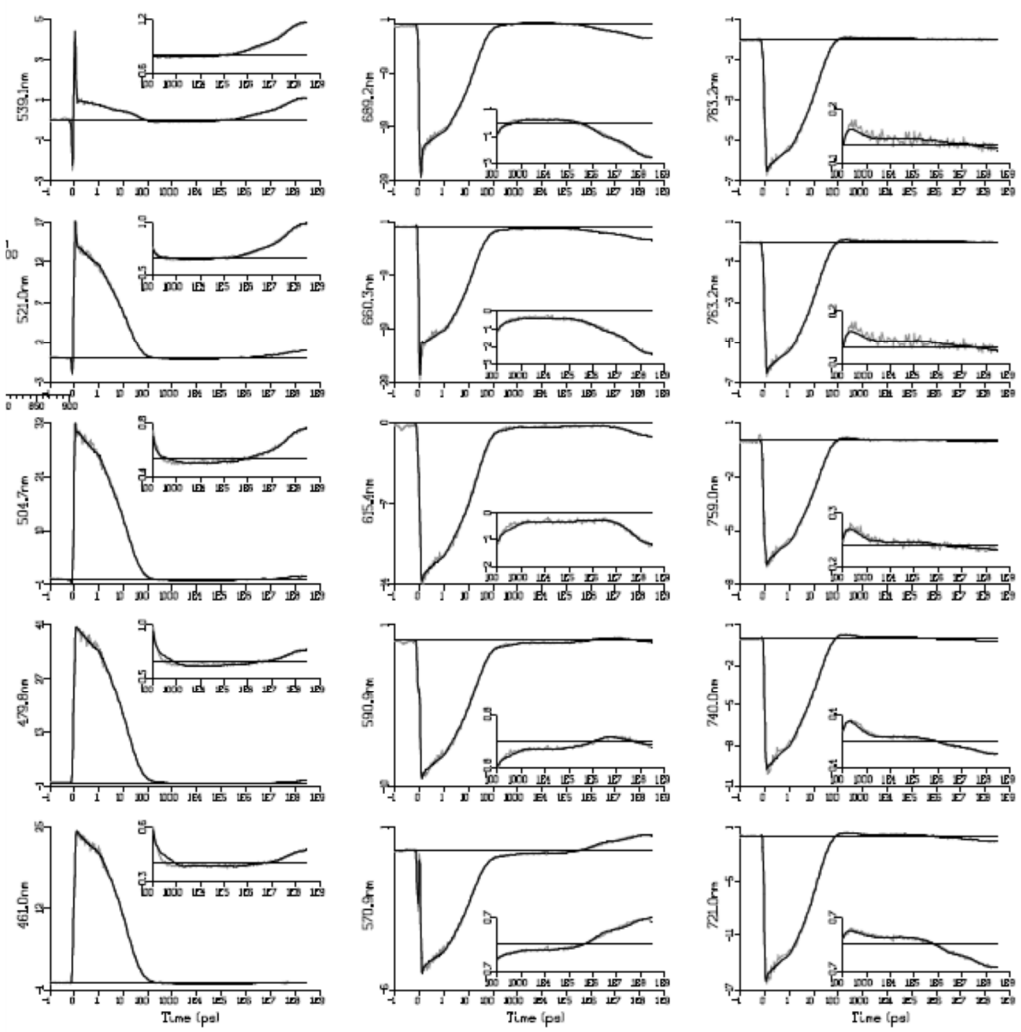

Fig. S4D. TA kinetic traces at selected wavelengths along with the result of the target analysis fit. Horizontal axes from fs - sub-ms, vertical axes ΔA in mOD.

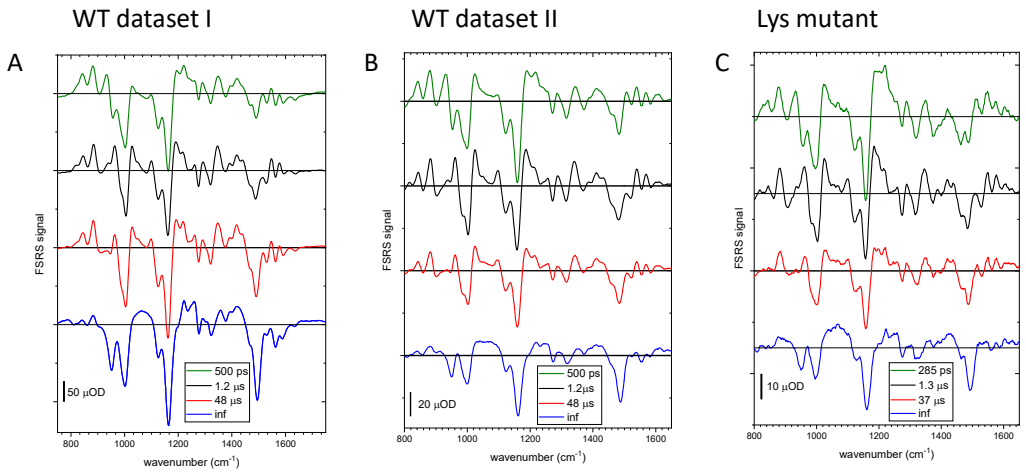

Fig. S5. EADS that follow from a sequential analysis of the FSRS data for (A) wild type, Dataset I, (B) wild type, Dataset II, and (C), Lys mutant, with time constants indicated in the panels.

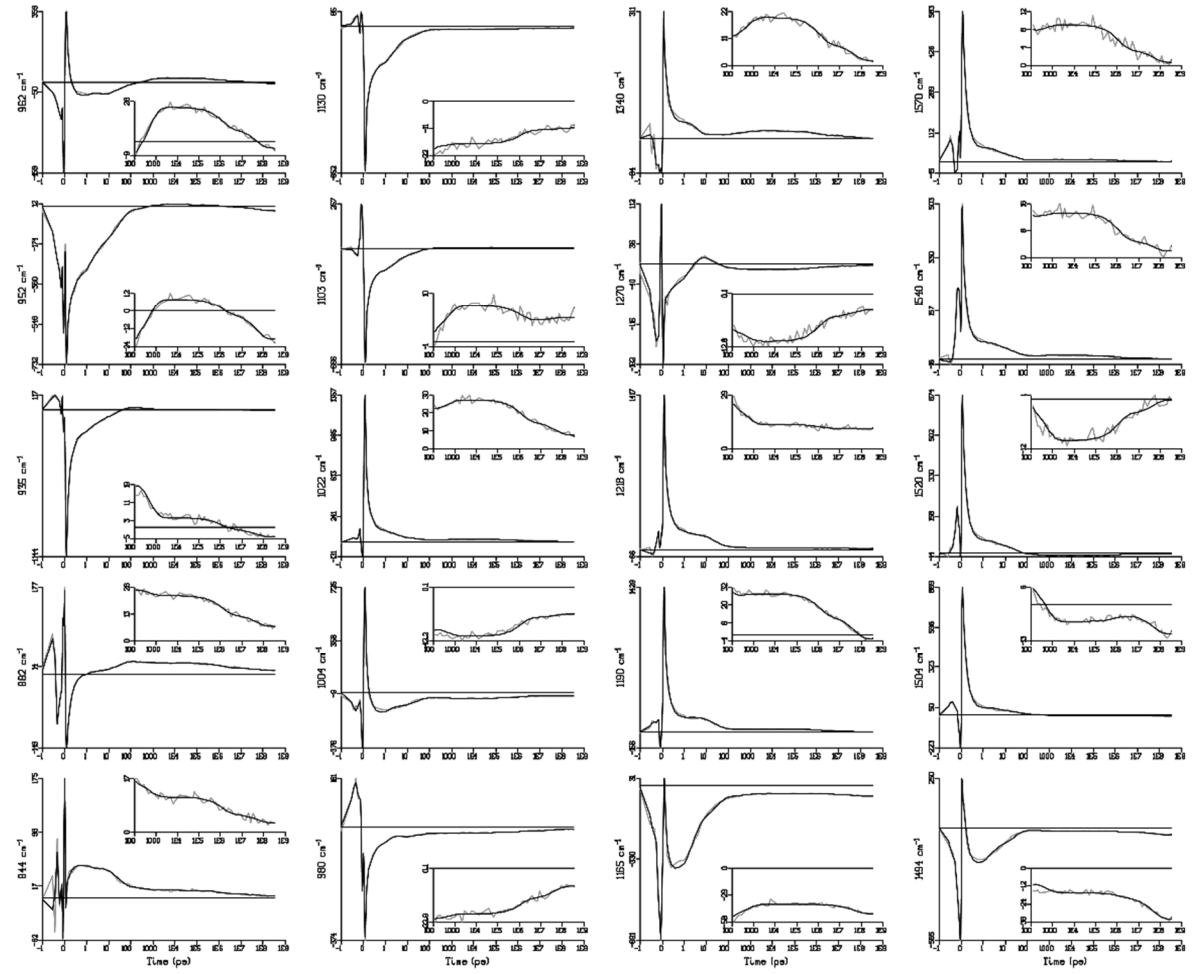

Figure S6. Selected time traces of the bestrhodopsin FSRS difference absorption (in µOD) of Dataset II at wavenumbers indicated in the ordinate label of the panels after 640 nm excitation. Key: data (grey) and fit (black). The overall rms error of the fit was 5.9 µOD. The time axis is linear until 1 ps and logarithmic thereafter. The insets show the kinetics after zoom after 100 ps to emphasize the product dynamics.

zoom after 100 ps is in the insets.

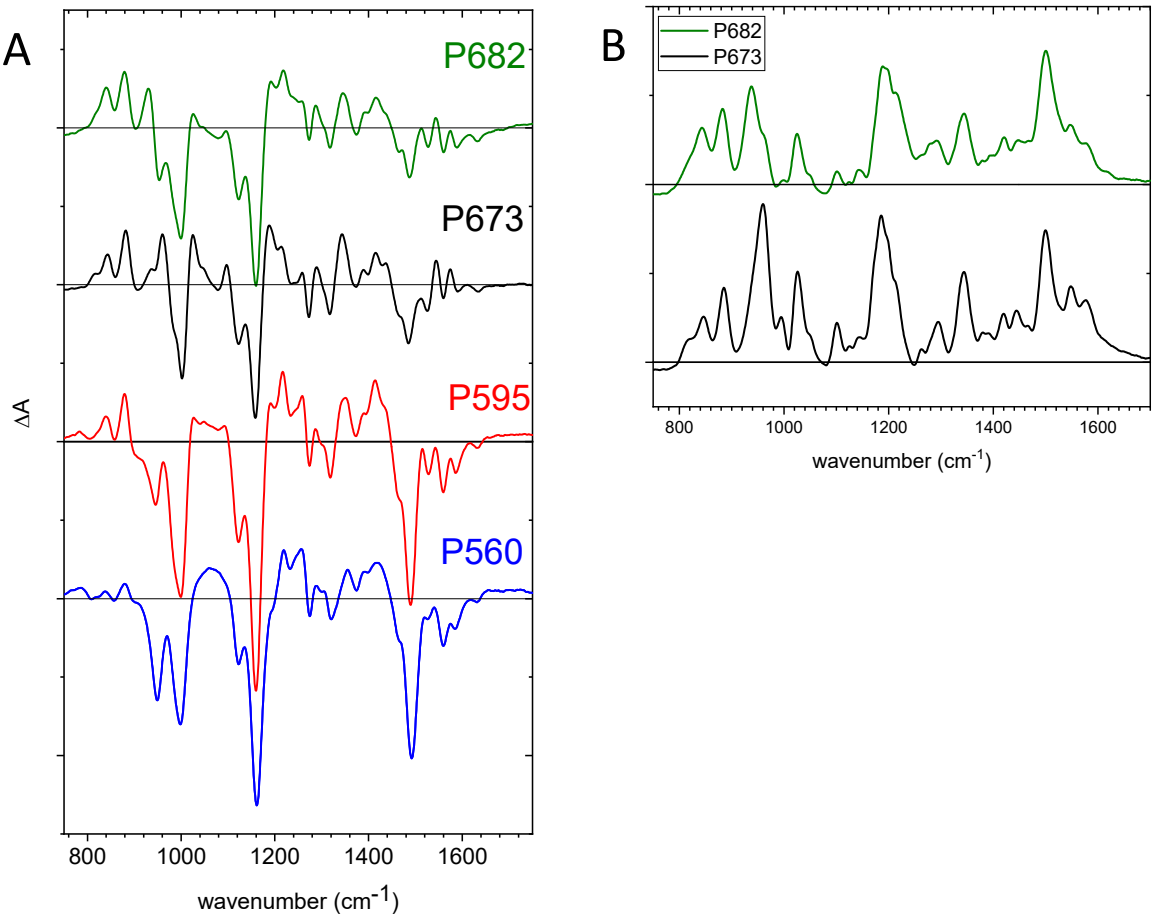

Fig. S7. (A) FSRS SADS from dataset I that follow from the equilibrium analysis of the model in Fig. S3C. (B) absolute spectra of P682 and P673 reconstructed from the SADS of panel (A).

Methods

Sample preparation

The tandemly arranged rhodopsin sequences (residues 1-786; GenBank: USH44360.1 derived from Phaeocystis Antarctica CCMP1374. The DNA provided by Dr. M. Shalev-Benami, Weizmann Institute of Science, Israel) was cloned into a pPICZ vector (Thermo Fisher Scientific, Waltham, MA, USA) with C-terminal StrepII-Tag. *Pichia pastoris* cells were transformed, and recombinant clones were selected according to the instructions of the manufacturer (Thermo Fisher Scientific, Waltham, MA, USA). Protein expression in buffered growth medium supplemented with 5 µM all-*trans* retinal was induced by adding 2.5% (v/v) methanol, and cells were harvested 24 h post-induction and lysed by a high-pressure homogenizer (HTU Digi-French-Press, G. Heinemann, Germany). The recombinant rhodopsin-tandem was solubilized from crude membrane fraction with 1.5% (w/v) dodecylmaltoside (DDM, Glycon, Luckenwalde, Germany) in HBS-buffer (50 mM HEPES pH 7.4, 100 mM NaCl). The protein was purified by affinity-chromatography using a 5 ml Strep-Tactin®XT Superflow® column (IBA GmbH, Göttingen, Germany), washed with 50 ml of washing buffer (50 mM HEPES (pH 7.4), 100 mM NaCl, 0.02% DDM), and eluted with 2X BTX-buffer containing 100 mM biotin (IBA GmbH) and supplemented with 0.02% DDM. Colored fractions were pooled and concentrated in a washing buffer (Amicon Ultra Centrifugal Filter, molecular weight cutoff (MWCO) 100 kDa, Merck Millipore, Burlington, MA, USA). The lysine mutant (K332A) was obtained by site-directed mutagenesis (using the following Primers: GACGTGGTCATGGCGCTGTCCCACACC; GGTGTGGGACAGCGCCATGACCACGTC), then further prepared and measured analog to the wildtype.

Transient absorption spectroscopy

All time-resolved-spectroscopy experiments were conducted on a homebuilt 1-kHz transient absorption (TA) and femtosecond-stimulated Raman spectroscopy (FSRS) set-ups constructed around femtosecond titanium:sapphire amplifiers Femtopower (Spectra Physics) and Solstice amplifier (Spectra Physics) sharing a common oscillator. The amplifiers were synchronized both by means of electronic triggering and optical delay of the seed prior to amplification, which allows for setting the delay between their pulses up to <1 ms with femtosecond precision. In the TA experiment two laser beams were employed, pump and probe. A white light supercontinuum generated in an Argon-filled hollow core fiber (Ultrafast Innovations, Savannah, USA) driven by the Femtopower amplifier served as the probe. The pump beam (centered on 700 nm, 18 nJ per pulse) was generated by an optical parametric amplifier (OPA) (TOPAS, Light Conversion, Vilnius, Lithuania) driven by the Solstice amplifier. Pump and probe beams were overlapped and focused at the same spot in the sample. Each beam was interrupted on shot-to-shot basis by an optomechanical chopper to acquire all four possible pulse combinations (pumped, not-pumped, dark background, pump-only). The spectrum of the probe beam transmitted through the sample was acquired by a home-built prism spectrometer utilizing 1 kHz CCD camera (Entwicklungsbuero Stresing, Berlin, Germany). In order to reduce the noise due to white light fluctuations we used a second identical detector to acquire a reference spectrum of the probe replica avoiding the sample and we performed a correction as described in (9). During all experiments the sample was kept in a 1-mm thick optical cell. The common focus of laser beams was randomly scanned across the sample surface in order to replenish fresh sample. Additionally, the

sample was continuously illuminated with a green LED in order to facilitate the bestrhodopsin back conversion into its D661 original state. 361 exponentially spaced time delays from 10 femtoseconds to 0.6 milliseconds were implemented to sample the photoinduced dynamics of Bestrhodopsin. All the experiments were taken under the magic angle (54.7°) condition to remove the influence of orientation relaxation.

Flash photolysis spectroscopy

Sub-microsecond-to-second transient absorption spectra (flash photolysis) were obtained with LKS.60 flash photolysis system (Applied Photophysics Ltd, Leatherhead, UK) equipped with a tunable optical parametric oscillator (MagicPrism, Opotek Inc., Carlsbad, CA, USA) pumped by the third harmonic of an Nd:YAG laser (Brilliant B, Quantel, Les Ulis, France). The protein was excited with a 10 ns laser pulse, adjusted to 660 nm, and probed by the light of a short-arc XBO Xenon lamp (150 W, Osram, München, Germany). The transient absorbance changes (10 ns – 0.1 s) were detected by an Andor iStar ICCD Camera (DH734, Andor Technology, Belfast, Northern Ireland), and the data was averaged over 20 cycles. Photo-induced back conversion to D661 was achieved by illuminating the sample for ~1 s with 530 nm LED light after each taken spectrum.

Femtosecond stimulated Raman spectroscopy

The femtosecond-stimulated Raman spectroscopy setup is an upgraded version (10) of the one described in our previous work (11). In the current design, we seeded two independent 1 kHz chirped pulse amplifiers (CPAs) with femtosecond pulses from one shared Ti: sapphire oscillator. We delayed the seed electronically and optically to trace processes beyond six nanoseconds. To initiate a photoreaction, we employed pulses of 150 nJ at 650 nm (dataset I) or 50 nJ at 650 m (dataset II and Lys mutant) from the OPA driven by the Solstice amplifier focused into a 100 µm spot as the actinic pump. Actinic pulse duration was about 50 fs (full width half maximum). Meanwhile, we focused a 1450 nm signal beam from a second OPA system on a moving CaF_2 plate to generate a white light supercontinuum as the probe, and the probe was focused on the sample at a spot of approximately 50 µm. In the detection apparatus, the probe was split into two beams. One part was sent to a grating-based high resolution imaging spectrograph (Acton, Princeton instruments) for Raman analysis in the 750 nm to 950 nm region. The other part was directed to a prism spectrograph to obtain transient absorption spectra in the 370 nm to 1200 nm range. In both spectrographs, a 58x1024 pixels CCD camera (Entwicklungsbuero Stresing) was used as a linear image sensor via operation in a full vertical binning mode. Cameras were triggered from the lasers at 1 kHz and provided shot-to-shot detection. The 800 nm femtosecond pulses from the second amplifier passed through a home-built pulse shaper to create a series of frequency-locked picosecond pulses as the Raman pump, totalling 96 wavelength-shifted Raman pumps. The energy of the Raman pump was 2 µJ (dataset I) or 1 µJ (dataset II and Lys mutant). We implemented 98 exponentially spaced time delays from 10 femtoseconds to 0.6 milliseconds to sample the photoinduced dynamics of bestrhodopsin. All the experiments were taken under the magic-angle (54.7°) condition to remove the influence of orientation relaxation. To reduce the impact of photodamage in the measurement, we moved the sample in the beam at a speed of approximately 10 cm/s in a sample scanner. The sample was contained in a cuvette is 1 mm path length and kept in the D661 state by background illumination with a green LED. The steady-state

stimulated Raman spectra were taken with the actinic pulse off. Here, D661 was prepared either through dark adaptation or via background illumination with a green LED. Steady-state P540 was prepared by illumination with a red LED, which resulted in a mixture of P540 (major contribution) and D661 (minor contribution). The P540 stimulated Raman spectrum was reconstructed from the data by appropriate subtraction of the D661 stimulated Raman spectrum fraction, and scaled in Fig. 2 to match the signal intensity of D661.

The absorption spectra was fitted as a function of the wavenumber with skewed gaussian shapes(12)

$$\varepsilon(\bar{\nu}) / \bar{\nu} = \varepsilon_{\max} \exp(-\ln(2)[\ln(1 + 2b(\bar{\nu} - \bar{\nu}_{\max}) / \Delta\bar{\nu}) / b]^2)$$

with parameters $\bar{\nu}_{\max}$, $\Delta\bar{\nu}$, and *b* for the location of the maximum, FWHM, and skewness.

1. I. Palings, E. M. M. Vandenberg, J. Lugtenburg, R. A. Mathies, COMPLETE ASSIGNMENT OF THE HYDROGEN OUT-OF-PLANE WAGGING VIBRATIONS OF BATHORHODOPSIN - CHROMOPHORE STRUCTURE AND ENERGY-STORAGE IN THE PRIMARY PHOTOPRODUCT OF VISION. *Biochemistry* **28**, 1498-1507 (1989).
2. I. H. M. Van Stokkum *et al.*, Reaction Dynamics in the Chrimson Channelrhodopsin: Observation of Product-State Evolution and Slow Diffusive Protein Motions. *Journal of Physical Chemistry Letters* (2023).
3. M. Braiman, R. Mathies, RESONANCE RAMAN-SPECTRA OF BACTERIORHODOPSINS PRIMARY PHOTOPRODUCT - EVIDENCE FOR A DISTORTED 13-CIS RETINAL CHROMOPHORE. *Proceedings of the National Academy of Sciences of the United States of America-Biological Sciences* **79**, 403-407 (1982).
4. S. O. Smith, J. A. Pardoen, J. Lugtenburg, R. A. Mathies, VIBRATIONAL ANALYSIS OF THE 13-CIS-RETINAL CHROMOPHORE IN DARK-ADAPTED BACTERIORHODOPSIN. *Journal of Physical Chemistry* **91**, 804-819 (1987).
5. K. Kajimoto *et al.*, Transient Resonance Raman Spectroscopy of a Light-Driven Sodium-Ion-Pump Rhodopsin from Indibacter alkaliphilus. *Journal of Physical Chemistry B* **121**, 4431-4437 (2017).
6. S. Shim, J. Dasgupta, R. A. Mathies, Femtosecond Time-Resolved Stimulated Raman Reveals the Birth of Bacteriorhodopsin's J and K Intermediates. *Journal of the American Chemical Society* **131**, 7592-7597 (2009).
7. G. Eyring, B. Curry, A. Broek, J. Lugtenburg, R. Mathies, ASSIGNMENT AND INTERPRETATION OF HYDROGEN OUT-OF-PLANE VIBRATIONS IN THE RESONANCE RAMAN-SPECTRA OF RHODOPSIN AND BATHORHODOPSIN. *Biochemistry* **21**, 384-393 (1982).
8. S. O. Smith *et al.*, VIBRATIONAL ANALYSIS OF THE ALL-TRANS-RETINAL CHROMOPHORE IN LIGHT-ADAPTED BACTERIORHODOPSIN. *Journal of the American Chemical Society* **109**, 3108-3125 (1987).
9. Y. Feng, I. Vinogradov, N. H. Ge, General noise suppression scheme with reference detection in heterodyne nonlinear spectroscopy. *Optics Express* **25**, 26262-26279 (2017).
10. Y. L. Liu *et al.*, Sub-Millisecond Photoinduced Dynamics of Free and EL222-Bound FMN by Stimulated Raman and Visible Absorption Spectroscopies. *Biomolecules* **13** (2023).

11. M. Kloz, J. Weissenborn, T. Polivka, H. A. Frank, J. T. M. Kennis, Spectral watermarking in femtosecond stimulated Raman spectroscopy: resolving the nature of the carotenoid S-star state. *Physical Chemistry Chemical Physics* **18**, 14619-14628 (2016).
12. I. H. M. van Stokkum, D. S. Larsen, R. van Grondelle, Global and target analysis of time-resolved spectra. *Biochimica Et Biophysica Acta-Bioenergetics* **1657**, 82-104 (2004).